Observation of Zero Current Density in the Core of JET Discharges with Lower Hybrid Heating and Current Drive

N. C. Hawkes,[1] B. C. Stratton,[2] T. Tala,[3] C. D. Challis,[1] G. Conway,[4] R. DeAngelis,[5] C. Giroud,[6] J. Hobirk,[4] E. Joffrin,[6] P. Lomas,[1] P. Lotte,[6] J. Mailloux,[1] D. Mazon,[6] E. Rachlew,[7] S. Reyes-Cortes,[8] E. Solano,[9] and K-D. Zastrow[1]

[1]*Euratom/UKAEA Fusion Association, Culham Science Centre, Abingdon, Oxfordshire, OX14 3DB, United Kingdom*
[2]*Princeton Plasma Physics Laboratory, P.O. Box 451, Princeton, New Jersey 08543*
[3]*Association Euratom-Tekes, VTT Chemical Technology, Espoo, P.O. Box 1404, Finland*
[4]*Max-Planck-Institut für Plasmaphysik, Euratom Association, 85740, Garching, Germany*
[5]*Association Euratom-ENEA sulla Fusione, CRE Frascati, Roma, Italy*
[6]*Association Euratom-CEA, CEA-Cadarache, F-13108 St. Paul lez Durance, France*
[7]*Euratom-NFR, Department of Physics 1, Royal Institute of Technology, SE 10044, Stockholm, Sweden*
[8]*Euratom/IST Association, Centro de Fusao Nuclear, 1049-001, Lisboa, Portugal*
[9]*Association EURATOM-CIEMAT para Fusion, CIEMAT, Madrid, Spain*
and EFDA CSU JET, Abingdon, OX14 3EA, United Kingdom
(Received 16 April 2001; published 22 August 2001)

Simultaneous current ramping and application of lower hybrid heating and current drive (LHCD) have produced a region with zero current density within measurement errors in the core ($r/a \leq 0.2$) of JET tokamak optimized shear discharges. The reduction of core current density is consistent with a simple physical explanation and numerical simulations of radial current diffusion including the effects of LHCD. However, the core current density is clamped at zero, indicating the existence of a physical mechanism which prevents it from becoming negative.

Tokamak experiments [1–3] have shown that heat and particle confinement in the plasma core can be improved by the presence of an internal transport barrier (ITB), motivating extensive study of plasma regimes with ITBs. (Reference [3] contains additional references to experimental work.) An important parameter determining the stability and confinement of the plasma is the safety factor, q, defined as the change of toroidal flux with poloidal flux, $\partial\Phi/\partial\psi$. ITBs can form most easily when the magnetic shear [$s \equiv (r/q)(dq/dr)$] is low or negative in the core region of the discharge [1–3]. The equilibrium state of the plasma current density profile, $j(R, Z)$, in an inductively driven discharge is peaked at the magnetic axis, where the temperature is highest and the resistivity is therefore lowest, resulting in positive shear everywhere in the plasma. [R is the major radius of the torus and Z is the distance from the plasma equatorial plane. In the following, $j(R, Z = 0)$ is denoted $j(R)$.] A standard technique for transiently obtaining low or negative shear is to inject neutral beam or radio frequency heating early in the discharge while the plasma current is ramping up. The heating increases the current diffusion time by decreasing the plasma resistivity, leading to $j(R)$ profiles that are flat or hollow due to current accumulation in the outer region of the plasma. In the JET tokamak, this results in q profiles that are approximately flat [$(q_0 - q_{min}) < 0.5$], with $q > 1$ everywhere, or low shear. During a subsequent high-power heating phase, ITBs often form near integer values of q, particularly $q = 2$ [3]. Recently, q profiles that are more strongly reversed [$0.5 < (q_0 - q_{min}) < 2$] have been obtained in JET by application of off-axis lower

hybrid heating and current drive (LHCD) during the current ramp-up, hereafter referred to as the LHCD prelude. In this scenario, the ITBs are not always linked to integer q values and the power threshold for ITB formation is lower than in standard optimized shear (OS) discharges [3]. An electron ITB can form early in the LHCD prelude, well before the high-power phase.

This Letter presents an observation of zero current density within measurement errors in the core ($r/a \leq 0.2$) of JET OS plasmas with a LHCD prelude. The magnetic field pitch angle in the plasma is measured by the motional stark effect (MSE) technique [4]. The MSE polarimeter observes D_α emission from energetic atoms injected with velocity $\mathbf{v}_b$ by the heating neutral beams. This emission is split into Stark components by the Lorentz electric field, $\mathbf{v}_b \times \mathbf{B}$, seen by the atoms due to their motion through the tokamak magnetic field, $\mathbf{B}$. The JET MSE polarimeter [5,6] measures the polarization angle of the π lines of the Stark spectrum, which are polarized parallel to the local electric field. The magnetic field pitch angle, $\gamma = \tan^{-1}(B_z/B_\phi)$, where B_z and B_ϕ are the vertical and toroidal components of $\mathbf{B}$, is deduced from the measured polarization angle of the D_α emission, γ_m, and is used as a constraint on magnetic equilibrium reconstructions. The statistical accuracy of the γ_m measurement is typically $\pm 0.1°$. The overall measurement error is typically $\pm 0.2°-0.3°$ when calibration uncertainties are included.

Figure 1 shows the time evolution of the plasma current, the LHCD and neutral beam injection (NBI) power levels, and the electron temperature, T_e, at two radii in a discharge that exhibited extreme shear reversal. This discharge had
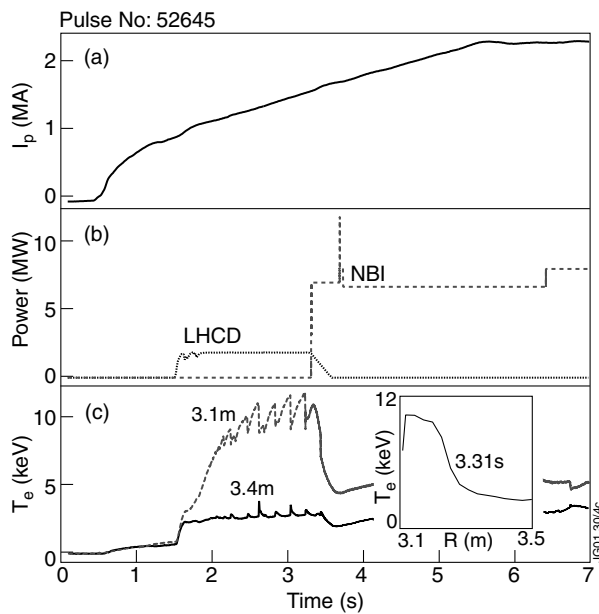
FIG. 1.   Time evolution of a JET discharge (No. 52645) that exhibited flat γ_m near the plasma axis at the end of the LHCD prelude. (a) Plasma current, (b) LHCD and NBI power levels, and (c) electron temperature at two radii (solid line: $R = 3.4$ m; dashed line: $R = 3.1$ m) showing sawtoothlike behavior associated with reversed shear.

FIG. 2.   Polarization angle, γ_m, measured with the MSE polarimeter at the end of the LHCD prelude in two similar discharges. Shot 52645 has a flat region of zero γ_m around the magnetic axis, indicating zero current density in this region, while shot 52631 does not show this effect.

a toroidal magnetic field, B_ϕ, of 2.6 T and plasma current, I_p, of 2.2 MA during the flattop. The LHCD power was 1.9 MW and the launcher was phased to drive current in the same direction as the plasma current (co-current drive). The T_e data show the sawtoothlike behavior often seen in discharges with a LHCD prelude and which is associated with shear reversal [3]. The core T_e shows a significant gradient (-100 keV m^{-1}), indicating that an electron ITB exists early in the LHCD prelude.

Figure 2 shows the MSE polarimeter measurement of the γ_m profile 4.0 s into the discharge, shortly after the end of the LHCD pulse and early in the NBI pulse. γ_m is flat over a region of $r/a \leq 0.2$ around the plasma axis and is zero within measurement errors. The fact that γ_m becomes zero over an extended region indicates that there is a portion of the plasma where $j(R)$ is zero within measurement errors. This feature in the γ_m profile has been seen on a large number of discharges with a LHCD prelude. In general, it is not possible to obtain MSE measurements at earlier times because the density is too low to permit neutral beam injection. However, in a few discharges, short beam pulses were injected as early as 2.5 s, during the time that a clear ITB was apparent in the T_e profiles. In these cases a flat region was again found to be present in the γ_m profile. In such a discharge, when the LHCD was not applied, no flat region in γ_m was measured and no sawtoothing behavior was present on T_e. Figure 2 also shows the γ_m profile measured in a discharge with a LHCD prelude that does not show the flat region near the plasma axis or evidence of a transport barrier in T_e. The formation of
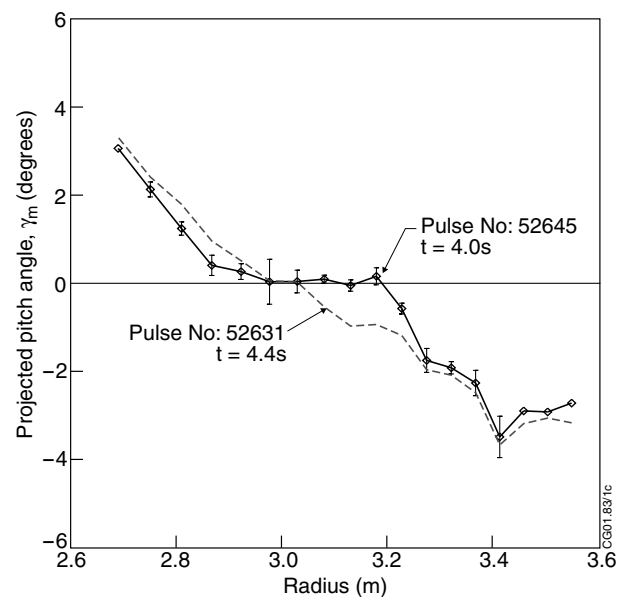
the flat region in γ_m during the LHCD prelude is sensitive to unresolved details of the evolution of $j(R)$ and n_e in the first 1 s of the discharge.

The radial component of the plasma electric field, E_r, can contribute to γ_m [7]. The magnitude of this effect was estimated for this discharge by using the value of E_r obtained from the radial force balance equation for carbon impurity ions and charge exchange spectroscopy measurements of the carbon ion temperature, density, and toroidal flow speed. A neoclassical estimate of the poloidal velocity is used [8]. At the time of the profiles shown in Fig. 2 the effect of plasma E_r changes the measured γ_m by $\sim0.2°$ (due mainly to the toroidal rotation term). A correction was applied to remove this effect from the profiles.

Under the usual discharge conditions of a positive current density everywhere in the plasma, the equilibrium can be described by the Grad-Shafranov equation with the flux surfaces labeled by the normalized poloidal flux, ψ [9]. However, for a plasma with zero current density over a particular region, ψ is also constant in this region. In this situation, ψ is not a monotonic, univalued variable and the equilibrium cannot be accurately reconstructed using the γ_m profile as a constraint in a magnetic equilibrium code which uses ψ as the independent variable. However, the vertical component of the magnetic field, B_z, can be estimated from γ. The value of γ is obtained from the measured pitch angle, γ_m, using an expression based on the full JET neutral beam and MSE polarimeter geometry [5]. This analysis shows that, like γ_m, B_z is near zero over the range $2.9 < R < 3.2$ m. The fact that B_z falls to

zero away from the plasma axis implies that there is a surface that encloses a significant region of zero total current. Since the MSE measurements extend across the diameter of this region, but do not give full coverage in the vertical direction, it is possible that opposed currents of equal magnitude could be flowing in the upper and lower parts of this region, giving, for example, two magnetic axes. However, there is no evidence from the soft x-ray camera data that the plasma has such a structure (the emission profiles are flat within errors) and we therefore conclude that the plasma current is zero across the whole of this region. Assuming, then, that the equilibrium is axisymmetric, the profile of $j(R)$ can be estimated from Ampère's law in a cylindrical geometry (r, θ, z) with θ being the poloidal angle.

Figure 3a shows the $j(R)$ profile calculated in this way from the γ_m profile of Fig. 2 (shot 52645). The current density in the plasma core is zero within an uncertainty of ± 0.2 MA m^{-2} derived from the γ_m measurement errors. This analysis was applied to other discharges that exhibited the flat γ_m region, and the zero core current is consistently seen. In general, measured γ_m profiles which exhibit the flat region do not appear to be consistent with negative values of the core $j(R)$. By ignoring the flat γ_m region, it was possible to obtain an approximate magnetic equilibrium reconstruction using the γ_m profile outside the zero-angle region as a constraint in the EFIT magnetic equilibrium re-

construction code [9]. The q profile obtained in this way was then modified by the difference between the calculated and measured values of B_z to obtain the approximate q profile shown in Fig. 3b. Because q becomes extremely large as $j(R)$ approaches zero, the rotational transform, $\iota = 1/q$, shown in Fig. 3c is a more appropriate description of these equilibria.

A region of zero or even negative $j(R)$ in the core can exist because the total flux, and therefore the total current, in the core of a highly conductive plasma cannot be rapidly modified due to slow radial diffusion of the parallel electric field [10,11]. This can be seen from the following expression, obtained by combining the radial derivative of Faraday's law with the time derivative of Ampère's law in cylindrical geometry and then eliminating the axial electric field using Ohm's law:

$$\frac{\partial j_{\text{tot}}}{\partial t} = \mu_0^{-1}\left(\frac{\partial^2}{\partial r^2} + \frac{1}{r}\frac{\partial}{\partial r}\right)\eta_{\parallel}(j_{\text{tot}} - j_{\text{ext}}).$$

Here, j_{tot} is the total parallel current density, j_{ext} is the externally driven (noninductive) parallel current density, and $\eta_{\parallel}$ is the parallel resistivity. Initially the external current drive is switched off ($j_{\text{ext}} = 0$) and the Ohmic current density, $j_{\text{tot}} - j_{\text{ext}}$, is nearly zero in the core and does not have a strong gradient. When the external off-axis current drive turns on, regions of positive radial curvature on either side of the peak in j_{ext} transiently decrease j_{tot}. With sufficient external current, this effect can locally drive the current density to zero or even negative. This situation can persist for many seconds in hot JET plasmas due to the long current diffusion time.

This effect can be seen in a simulation of the evolution of the flux surface averaged current density, $J(R)$, in this discharge performed using the JETTO transport code [12] with the assumption of neoclassical resistivity. Measured values of the densities, temperatures, Z_{eff}, plasma current, and magnetic field were used. The simulation was started at 1.0 s and the initial q profile was taken from an EFIT equilibrium constrained by external magnetic measurements only. The LHCD power deposition and generated current density are sensitive to the input temperature and density profiles, and the ray tracing is sensitive to the poloidal magnetic field, B_θ, so the fast ray tracing code [13] used to calculate the power deposition was run inside JETTO to provide a self-consistent model [14]. The beam-driven current is calculated with the PENCIL code [15] which is self-consistently coupled to JETTO.

Figure 4 shows the simulated $J(R)$ profiles at two times: (4a) during the LHCD prelude (3.0 s) and (4b) immediately after the LHCD prelude (4.0 s), when the MSE measurements were made. The contributions to the total current due to LHCD, Ohmic current, bootstrap current, and beam-driven current are shown. Figure 4a shows the region of zero $J(R)$ in the core region ($r/a \leq 0.2$) created in response to the strong off-axis LHCD. Note the wide region of negative Ohmic current due to the effect
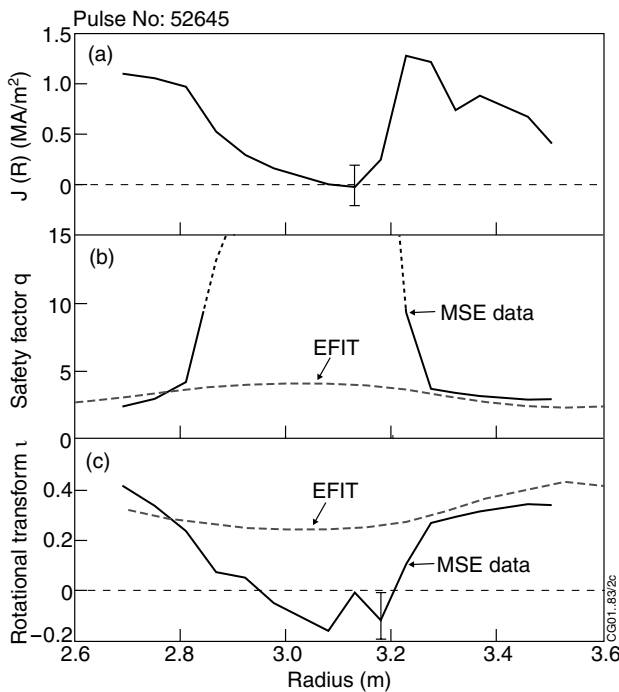
FIG. 3. (a) Current density profile, $j(R)$, derived from the MSE γ_m profile shown in Fig. 2 (No. 52645). (b) Solid lines: safety factor profile, $q(R)$, derived from γ_m measurement and approximate equilibrium solution for the outer region; dashed lines: approximate equilibrium solution for the outer region. (c) Profiles of $\iota = 1/q$ from γ_m measurement and approximate equilibrium solution.
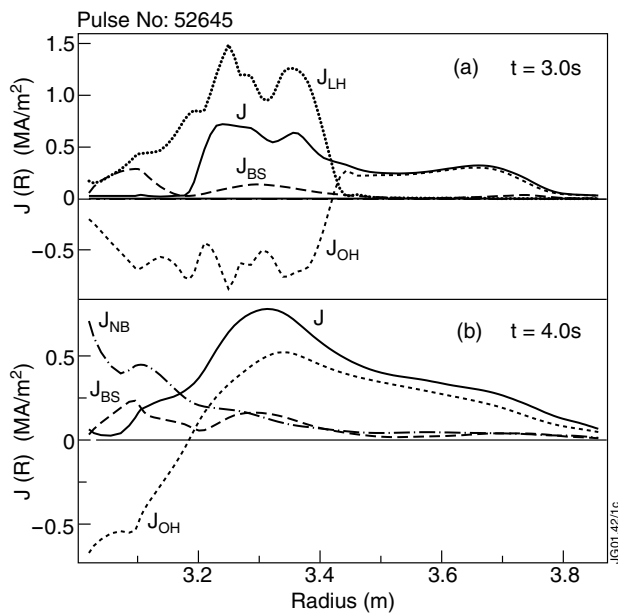
FIG. 4. JETTO code simulation of $J(R)$ in discharge shown in Figs. 1–3 at two times: (a) during the LHCD prelude (3.0 s; $J_{NB} = 0$) and (b) immediately after the LHCD prelude (4.0 s; $J_{LH} = 0$), when MSE measurements were made. The contributions to the total current due to LHCD (J_{LH}), Ohmic current (J_{OH}), bootstrap current (J_{BS}), and beam-driven current (J_{NB}) are shown. The region of zero core $J(R)$ due to LHCD is clearly seen in (a). The $J(R)$ profile shown in (b) is consistent with the $j(R)$ profile deduced from MSE measurements (Fig. 3a).

described above. As seen in Fig. 4b, the region of zero current begins to fill in after the LHCD turns off, leaving a small region of zero current density similar to that deduced from the MSE measurements (Fig. 3a). Shrinking of the region of zero current is significantly enhanced by the on-axis current driven by the neutral beams present at 4.0 s (Fig. 4b) but not at 3.0 s (Fig. 4a). The modeling is qualitatively consistent with the MSE measurements. The primary sources of uncertainty in the modeling are uncertainties in the measured input parameters, particularly the initial q and T_e. The resistivity, LHCD deposition, and bootstrap current profile calculations are not valid in the regime where the toroidal current vanishes [this situation is avoided by enforcing $q(r) < 60$]. However, the fact that this condition is attained in the code is a confirmation of the mechanism suggested as responsible for the zero axis current, while the profiles away from the zero current region will still be valid.

An examination of measured γ_m profiles in many discharges with an LHCD prelude does not show clear evi-

dence that the core $j(R)$ falls below zero, while the physical explanation and modeling discussed above indicate that this is possible. This observation suggests that a separate physical mechanism acts to prevent a negative core $j(R)$. The sawtoothlike MHD modes present during the LHCD prelude occur at the steep shear region, not in the zero current density region. It is possible that these modes could redistribute current from the periphery of the zero $j(R)$ region, preventing formation of a negative $j(R)$ region, but this has not yet been studied experimentally. The effect of these modes on $j(R)$ could be studied in a future experiment by correlating them with the time evolution of the γ_m profile.

A plasma regime with a region of zero core $j(R)$ suggests other interesting experiments. For example, it would allow neoclassical theory [16] to be tested in conditions of near zero B_θ. It would also allow the dependence of the $\mathbf{E} \times \mathbf{B}$ shearing rate on $\partial B_\theta / \partial r$ [17], and its effect on the ion thermal diffusivity, to be studied in a unique regime.

[1] F. M. Levinton et al., Phys. Rev. Lett. **75**, 4417 (1995).
[2] E. J. Strait et al., Phys. Rev. Lett. **75**, 4421 (1995).
[3] C. D. Challis et al., Plasma Phys. Controlled Fusion **43**, 861 (2001).
[4] F. M. Levinton et al., Phys. Rev. Lett. **63**, 2060 (1989).
[5] N. C. Hawkes et al., Rev. Sci. Instrum. **70**, 894 (1999).
[6] B. C. Stratton et al., Rev. Sci. Instrum. **70**, 898 (1999).
[7] M. C. Zarnstorff et al., Phys. Plasmas **4**, 1097 (1997).
[8] Y. B. Kim et al., Phys. Fluids B **3**, 2050 (1991).
[9] L. Lao et al., Nucl. Fusion **25**, 1611 (1985).
[10] Ya. I. Kolesnichenko et al., in *Reviews of Plasma Physics,* edited by B. B. Kadomtsev (Plenum, New York, 1992), Vol. 17, pp. 1–191.
[11] P. I. Strand and W. A. Houlberg, Phys. Plasmas **8**, 2782 (2001).
[12] G. Genacchi and A. Taroni, ENEA Report No. ENEA RT/TIB 1988(5), 1988 (unpublished).
[13] A. R. Esterkin and A. D. Piliya, Nucl. Fusion **36**, 1501 (1996).
[14] T. Tala et al., Nucl. Fusion **40**, 1635 (2000).
[15] C. D. Challis et al., Nucl. Fusion **29**, 563 (1989).
[16] Z. Lin et al., Phys. Plasmas **4**, 1707 (1997).
[17] E. J. Synakowski et al., Phys. Plasmas **4**, 1736 (1997).